

International Journal of Applied Mathematics in Control Engineering

Journal homepage: <http://www.ijamce.com>

Extraction of the Main Features of Pellet by Different Mathematical Algorithms

Yunxi Zhuansun^{a,*}, Jianming Zhi^b, Wei Zhang^a, Yang Han^{a,b}^a College of Science, North China University of Science and Technology, Tangshan, China.^b College of Metallurgy, North China University of Science and Technology, Tangshan, China.

ARTICLE INFO

Article history:

Received 1 May 2020

Accepted 5 July 2020

Available online 10 July 2020

Keywords:

Pellet ore phase

Gray level Co-occurrence Matrix

Box counting dimension

RGB color image histogram

ABSTRACT

Pellet ore is one of the important raw materials for blast furnace ironmaking. Its metallurgical properties at high temperature are important indexes for evaluating the quality of charge. Therefore, the quality inspection of pellet ore is an essential link for its furnace entry. From the point of view that the metallurgical properties of pellets determine their microstructure, and the microstructure reflects their metallurgical properties, the mineral phase characteristics at different locations of pellets are explored, and the relationship between the mineral phase characteristics and alkalinity is established, which has important guiding significance for the actual production of pellets. By comparing the pellet images with different visual features, this paper intends to study the texture features, fractal features and color features of the pellet phases by using three methods: Gray level Co-occurrence Matrix, Box counting dimension and RGB histogram. The texture feature extraction model, Box Counting Dimension fractal feature extraction model and RGB histogram color feature extraction model of grey symbiosis matrix were established respectively. Finally, the texture feature, fractal feature and color feature can be used as the basis of basicity, position and element identification of pellets.

Published by Y.X.Union. All rights reserved.

1. Introduction

Pelletite is one of the important raw materials for blast furnace ironmaking, with high iron-containing taste, uniform particle size, good reduction performance, high mechanical strength, and many micropores[1],[2]. In recent years, there are not many relevant literatures for studying the mineral phase of pellets. Professor Manchu Chu of the School of Materials and Metallurgy of Northeastern University and others have studied the effect of pre-oxidation experiments on the mineral phase and internal structure of pellets. It is verified that with the process of pre-oxidation, the cubic crystal lattice wants to change the crystal form of the six-sided lattice, which causes the pellets to shrink[3],[4]. In recent years, at home and abroad, it is generally recognized that good metallurgical performance of pellets at high temperature is an important indicator for evaluating the quality of the charge, and the metallurgical properties of pellets are closely related to their microstructure. Therefore, from the perspective of pellets metallurgical performance, explore pellets The characteristics of the mineralogy at different locations of the mine establish the relationship between the mineralogical features and the alkalinity, which has important guiding significance for the actual production of pellets[5],[6]. In this paper, the image

graphics processing algorithm is used to study the pellet phases contained in the attachment and extract the visual characteristics of all mineral phases. The longitudinal study of the variation gradients of various characteristics of the pellet phases at the same location under four alkalinities and extraction It can characterize the main characteristics of the mineral phase of the pellet alkalinity and realize the basicity discrimination based on the main feature. The horizontal study of the gradient of various characteristics of the pellet basic phase of the same alkalinity in three parts, and the extraction can be characterized. The main characteristics of the mineral phase of the agglomerate part, to achieve the location identification based on the main feature. Based on the above research, to determine the basicity category and location category of the 24 pellet ore phase given in Figure 7.

The main structure of this paper is as follows:

A texture feature extraction model based on gray co-occurrence matrix is established. Firstly, the energy, entropy, moment of inertia and correlation of gray level co-occurrence matrix are selected; Then, using MATLAB software to calculate the data of pellet mineral phase, and get the contrast chart of characteristic quantity under different basicity; Finally, the texture feature information is compared longitudinally, and the result shows that the texture feature can be used as the main

* Corresponding author.

E-mail addresses: zhuansunyunxi_ncst@163.com (Y. Zhuansun)

feature to judge the basicity.

A fractal feature extraction model based on box dimension is established. Firstly, the fractal dimension of the pictures in different parts of the same alkalinity and different parts of the same alkalinity is calculated by MATLAB; then, the result of dimension is drawn into line graph; Finally, the fractal feature information is compared horizontally, and the fractal feature can be used as the main feature to distinguish the location.

A color feature extraction model based on RGB color image histogram is established. Firstly, the color channels of different parts, alkalinity and elements are extracted; Then, the RGB primary colors of the seven extracted elements are compared, and the color feature contrast map is obtained; Finally, the color feature can be used as the main feature for element discrimination.

2. Texture feature extraction model based on gray co-occurrence matrix

Texture analysis is the extraction and analysis of spatial distribution pattern of image gray. Texture analysis is widely used in remote sensing image, X-ray photo, cell image interpretation and processing. There is no unified mathematical model for texture. It originated from the concept of texture which represents the surface properties of textiles. It can be used to describe the arrangement of any material components, such as lung texture in medical X-ray photos, blood vessel texture, lithology texture in aerospace (or aviation) topographic photos, etc. The visual texture in image processing is generally understood as the repeated arrangement of some basic patterns (tone primitives). Therefore, the description of a texture includes determining the hue primitives that make up the texture and determining the relationship between hue primitives. Texture is an area property, so it is related to the size and shape of the area. The boundary between the two texture modes can be determined by observing whether the texture measurement changes significantly. Texture is the reflection of the object structure. Analyzing texture can get the important information of the object in the image. It is an important means of image segmentation, feature extraction and classification recognition. For spatial domain image or transform domain image, we can use statistical and structural methods for texture analysis.

Statistical texture analysis is used to find the digital features that describe the texture, and these features or other non texture features are used to classify the regions in the image (rather than a single pixel). The autocorrelation function, gray level co-occurrence matrix, gray level run and various statistics of gray level distribution in local area of image are commonly used digital texture features. For example, the gray level co-occurrence matrix uses the spatial distribution of gray level to represent the texture. Because the gray distribution of coarse texture changes more slowly with distance than that of fine texture, they have totally different gray level co-occurrence matrix. Structural texture analysis studies the primitives of texture and their arrangement rules. A primitive can be either a pixel's gray level or a connected set of pixels with specific properties.

2.1 Basic principle of gray level co-occurrence

The concept of gray level co-occurrence matrix was put forward by Haralick in 1973. The gray histogram is the result of statistics on a single pixel on the image with a certain gray level, however, the gray level co-occurrence matrix is obtained by

statistically calculating the condition that two pixels at a certain distance on the image have a certain gray level[7]. The value of element (i, j) in the gray level co-occurrence matrix represents the number of times such two pixels appear in the image: one pixel has a gray value of i , the other pixel has a gray value of j , and the adjacent distance is d . The direction is θ (angle with the horizontal axis of the coordinate). The direction value is $0^\circ, 45^\circ, 90^\circ, 135^\circ$.

Let a be $f(x, y)$ two-dimensional digital image with the size of $M \times N$ and the gray level of L , the gray level co-occurrence matrix is the starting point of the pixel with $f(x, y)$ gray level as i , calculate that the gray level co-occurrence matrix that appears at the same time with pixel $(x+a, y+b)$ (Distance d , gray j) is $P(i, j, d, \theta)$, expressed as formula (1):

$$P(i, j, d, \theta) = \left\{ \left[(x, y), (x+a, y+b) \right] \Big|_{f(x+a, y+b)=j} \right\} \text{ among } \begin{cases} f(x, y) = i \\ x = 0, 1, 2, \dots, L_x - 1; y = 0, 1, 2, \dots, L_y - 1 \end{cases} \quad (1)$$

In the formula, X, Y is the pixel coordinates in the image; a, b is the offset; L_y, L_x is the number of rows and columns of the image.

Haralick derives 14 kinds of texture feature statistics from GLCM. Because there is a certain correlation between various statistics, it is not necessary to use all statistics for texture analysis. This article uses four characteristics of energy, entropy, moment of inertia and correlation. As the GLCM texture feature, the calculation formula of the four feature quantities [8],[9],[10]. As shown in Table 1.

Table 1. Summary table of characteristic quantities

Feature amount	Formula	Feature
Energy	$\sum_{i=1}^k \sum_{j=1}^k (G(i, j))^2$	The energy reflects the uniformity of the gray distribution of the image and the thickness of the texture.
Entropy	$\sum_{i,j} P_{\theta,d}(i, j) \log_2 P_{\theta,d}(i, j)$	The entropy value indicates the complexity of the grayscale distribution of the image. The larger the entropy value, the more complex the image.
Inertia	$(i - j)^2 P(i, j, \theta)$	The magnitude of the moment of inertia reflects the local change of the gray distribution.
Correlation	$\frac{\sum_{i,j} [(ab)P_{\theta,d}(a,b)] - \mu_i \mu_j}{\sigma_i \sigma_d}$	The correlation value reflects the local gray correlation in the image

2.2 Feature extraction of pellet mineral texture

The images of different alkalinities in different parts of the pellet phase are shown in Fig. 1. Based on the calculation of the gray level co-occurrence matrix feature in Table 1, 6 pellets are selected to compare the four characteristics in the case of different alkalinity and different parts Changes in magnitude. Using matlab software to calculate the feature quantity of the gray level co-occurrence matrix, you can get the energy, entropy,

moment of inertia and correlation under the same element, different parts, different alkalinity, different angles [11],[12].

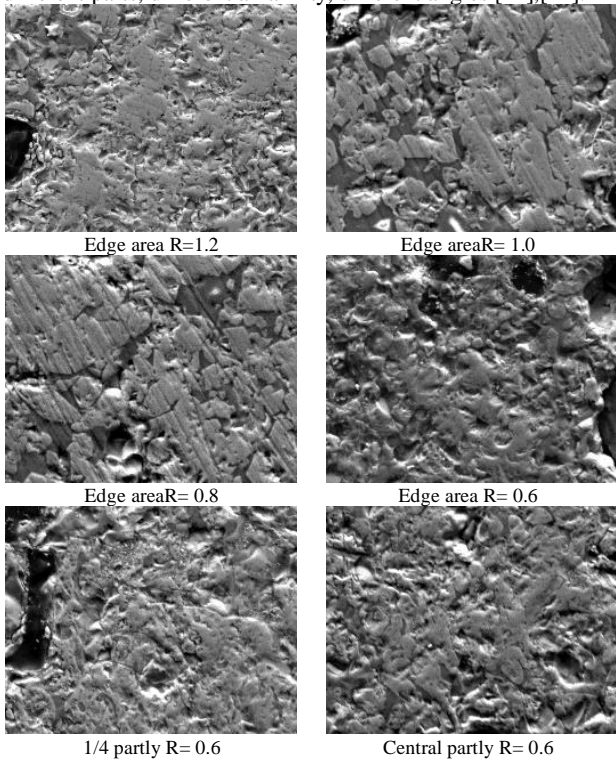


Fig. 1. Pelletite mineral phase picture.

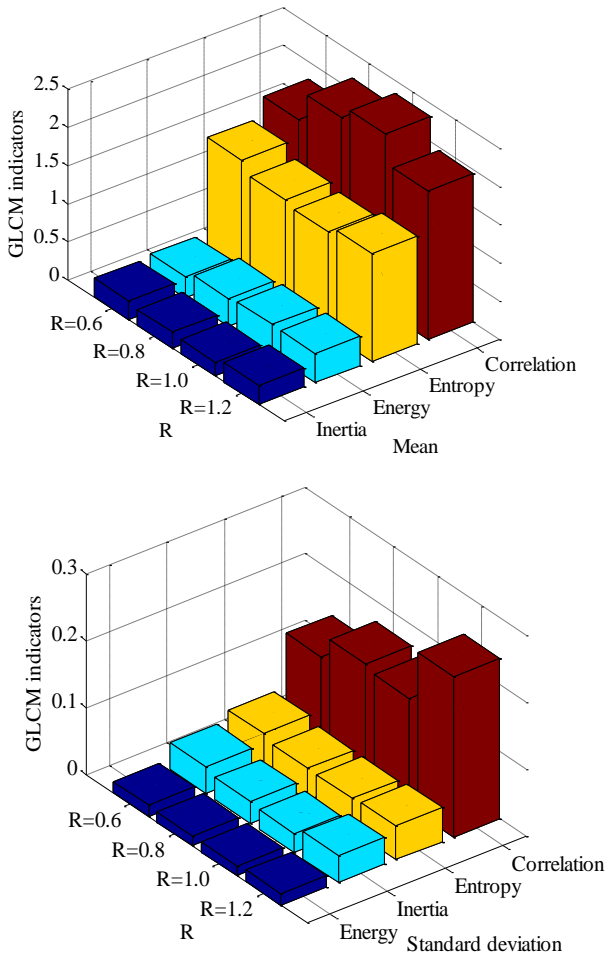


Fig. 2. Index of gray symbiosis matrix at the edge.

This article takes the edge of the original image as an

example to show the mean and standard deviation of energy, entropy, moment of inertia, and correlation at different alkalinities, as shown in Fig. 2.

Select energy, entropy, moment of inertia, and correlation as the four indexes of the gray level co-occurrence matrix, take the parameters of the four angles and the standard deviation to simulate the parameters of the gray level co-occurrence matrix, and make a longitudinal comparison between the indexes. The alkalinity of the four indicators is larger at 0.6 and 1.2, and smaller at 0.8 and 1.0. Extended use of curve fitting can predict the specific values of the four indicators with alkalinity above 1.2.

Similarly, complete the table of mean and standard deviation of energy, entropy, moment of inertia and correlation under different parts. By means of statistics of the mean and standard deviation of the data in the 6 tables, draw a comparison chart, as shown in Fig. 3 and Fig. 4 As shown

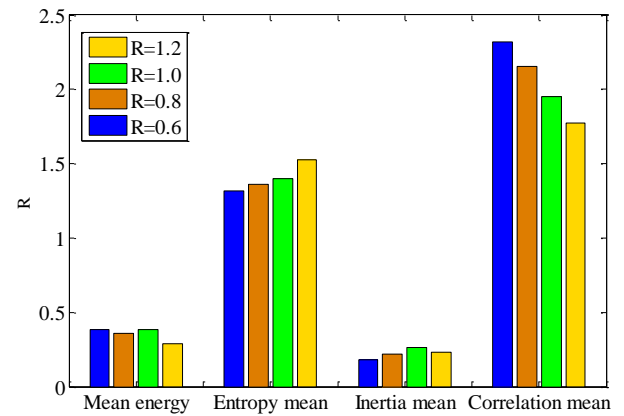


Fig. 3. Comparison of characteristic quantities at the edge

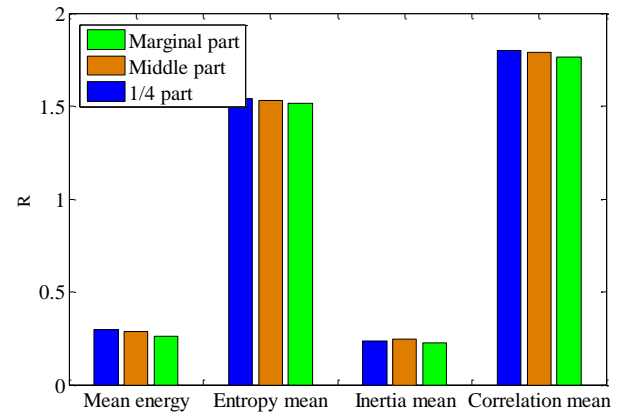


Fig. 4. Comparison of characteristic quantities under the same basicity when R=0.6

From Fig.3 and Fig. 4, we can see that under different alkalinity, the correlation value is the most significant as an indicator of texture characteristics. The texture characteristics of the pellet phase at the same basicity are not obvious. From this we can conclude that the texture features used to identify the same element at the same location and different alkalinity are more obvious, so to identify different alkalinity, the texture feature should be the main feature.

3. Fractal feature extraction model based on box counting dimension

3.1 Principle of counting box dimension

The concept of fractal was first proposed by the mathematician B. Mandelbrot [13],[14]. Fractal mainly refers to a system that is fragmented and complex but has self-similarity or

self-radioactivity. Fractal refers to the use of the characteristics of the ontology through irregular Explore the nature of the rules and solve practical problems.

Fractal theory is a very popular and active new theory and new subject in the world. In 1967, he published a famous paper entitled "how long is the coastline of Britain?" in the authoritative American magazine science. As a curve, the coastline is very irregular, very unsmooth, showing very complex changes. We can't distinguish the difference between this part of the coast and that part of the coast in terms of shape and structure. This almost the same degree of irregularity and complexity shows that the coastline is self similar in morphology, that is, the similarity between local morphology and overall morphology. When there is no building or other reference, the 100 kilometer coastline taken in the air will look very similar to the two photos of the 10 kilometer coastline enlarged.

In fact, self similar forms are widely found in nature, such as: continuous mountains and rivers, floating clouds, broken mouths of rocks, tracks of Brownian particles, crowns, cauliflower, cerebral cortex. Mandelbrot called these parts and the whole in some way similar to the shape of fractal. In 1975, he founded fractal geometry.

On this basis, the science of studying fractal properties and its application is formed, which is called fractal theory.

The significance of fractal theory. Fractal theory and its methodology are of great significance in scientific methodology. It breaks the separation between the whole and the part, the confusion and the rule, the order and the disorder, the simple and the complex, the limited and the infinite, the continuity and the discontinuity, finds the media and the bridge between them (that is, the similarity between the part and the whole), for people to know the rule and the order from the chaos and the disorder, the whole from the part and the whole from the limited The possibility and basis of understanding infinity are provided through infinite deepening and limited cognition; Together with system theory, self-organization theory, chaos theory and other scientific theories, it reveals the multi-level, multi perspective and multi-dimensional connection between the whole and part, chaos and rule, order and disorder, simple and complex, limited and infinite, continuous and interval, which makes people's thinking mode of understanding their relationship from linear stage to multi-dimensional stage Nonlinear stage.

Principles of fractal theory:

Self similar principle and iterative generation principle are important principles of fractal theory. It shows that fractal has invariance under the general geometric transformation that is scale independence. Since self similarity starts from symmetry of different scales, it means recursion. The self similarity of fractal body can be the same or the statistical similarity. Standard self similar fractals are mathematical abstractions, which generate infinite fine structures by iteration, such as Koch snow curve, Sierpinski carpet curve, etc. This kind of fractal is only a few, most of them are random fractal in statistical sense.

Fractal dimension, as a quantitative characterization and basic parameter of fractal, is another important principle of fractal theory. Fractal dimension, also known as fractal dimension or fractional dimension is usually represented by fraction or number with decimal point. For a long time, people are used to define point as zero dimensions, line as one dimension, plane as two dimensions and space as three dimensions. Einstein introduced time dimension into relativity, and then formed four-dimensional space-time. Considering a problem in many ways, we can establish high-dimensional space, but all of them are integer dimensions. In mathematics, the geometric objects of Euclidean space are continuously stretched, compressed and twisted, and the dimension is also unchanged, which is the topological dimension. However, this traditional view of dimension has been challenged. Mandelbrot once described the dimension of a rope ball: Observing the rope ball from a long distance can be regarded as a point (zero dimensions).

From a closer view, it is filled with a spherical space (three-dimensional); A little closer, you see the rope (one dimension); Further to the micro level, the rope becomes a three-dimensional column, and the three-dimensional column can be decomposed into one-dimensional fibers.

Fractal dimension is a crucial element in the fractal process. Common dimensions include similar dimension, Hausdorff dimension, box counting dimension, etc. Among them, box counting dimension is a commonly used fractal dimension method because it is easy to understand and easy to calculate [15]. This paper uses box counting dimension method to calculate the fractal dimension.

Box counting dimension is also called box dimension, which is defined as let F be any non-empty bounded subset in R^n , and let $N(F, \lambda)$ denote the maximum diameter as λ and the smallest number that can cover F set [16],[17]. Then the expressions of the upper and lower box dimensions of F are :

$$\dim_{Bax}^1 F = \lim_{\lambda \rightarrow 0} \frac{\ln N(F, \lambda)}{\ln(1/\lambda)} \tag{2}$$

$$\dim_{1Bax} F = \lim_{\lambda \rightarrow 0} \frac{\ln N(F, \lambda)}{\ln(1/\lambda)} \tag{3}$$

If the upper and lower box dimensions are equal, the box dimension of F is defined as:

$$\dim_{Bax} F = \lim_{\lambda \rightarrow 0} \frac{\ln N(F, \lambda)}{\ln(1/\lambda)} \tag{4}$$

Among them, $N(F, \lambda)$ can take one of the smallest number of cubes covering the side length of F for λ and the smallest number of sets covering the diameter of F at most λ .

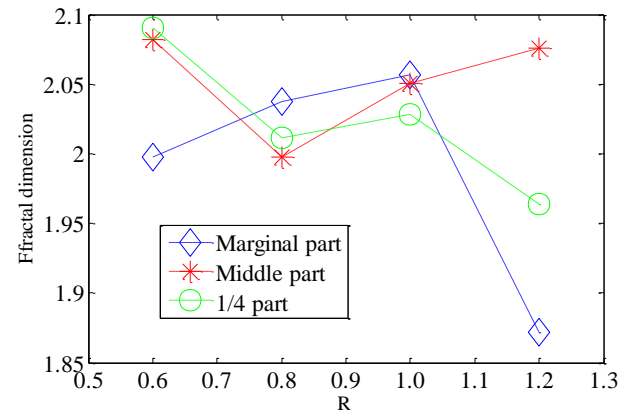


Fig. 5. Fractal dimension line chart of different basicity in the same part.

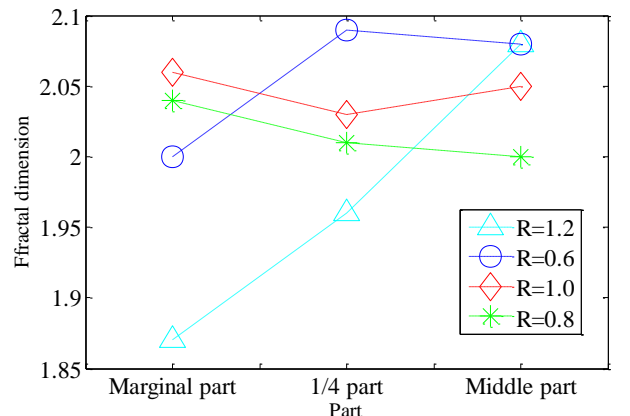


Fig.6. Fractal dimension line chart of different parts of the same basicity

First, grayscale the color image to get a grayscale image (because the image has been processed above, no explanation

will be given), and then use the box counting dimension method to calculate the fractal dimension [18].

3.2 Fractal feature extraction based on box counting dimension

Use Matlab to calculate the fractal dimension of the pictures located in different parts of the same basicity and different parts of the same basicity, and draw their line charts, as shown in Fig. 5 and Fig. 6.

From Fig. 5 and Fig.6, it can be seen that the central part of the mineral phase is more significant than the edge part and the quarter fractal dimension, and the alkalinity has little effect on the fractal dimension, that is, the fractal feature identifies the different parts of the same element The effect is the best, so the fractal feature can be used as the main feature to identify different parts of the pellet.

4. Color feature extraction model based on RGB color image histogram

The RGB color model is a color standard in industry today, various colors are obtained by changing the three color channels of red (R), green (G), and blue (B) and superimposing each other, RGB is the color representing three channels of red, green and blue. This standard includes almost all colors that human vision can perceive [19],[20]. It is one of the most widely used color systems at present.

RGB color space according to the actual use of different equipment system capabilities, there are different ways to achieve. As of 2006, the most commonly used method is 24 bit implementation, that is, each channel has 8-bit or 256 color level. The color space based on such a 24 bit RGB model can represent $256 \times 256 \times 256 = 16.7$ million colors. Some implementation methods use 16 bits per primary color, which can achieve higher and more accurate color density in the same range. This is particularly important in wide color spaces, where most commonly used colors are arranged relatively closely. as shown in Table 2.

Table 2. RGB description

Component	Description
R	Required parameter; Type Integer. Values range from 0 to 255, Representing the red component of the color.
G	Required parameter; Type Integer. Values range from 0 to 255, Representing the green component of the color.
B	Required parameter; Type Integer. Values range from 0 to 255, Representing the blue component of the color.

Note: if one of the parameters has a value greater than 255, no error is shown, but the parameter is treated as 255.

The color image is generally composed of three channels of RGB, each channel is composed of 8 bits, and the maximum is 255. If the histogram is directly constructed according to each different value of the three channels, it is very large first, including $256 \times 256 \times 256$ bins. For simplicity, each channel is set with 8 bins. In this way, the maximum value of each channel is $256/8=32$, that is, each channel is divided into 8 bins, and each bin can store 32 numbers, 0-31,32-63 , 64-127, ... 224-255, etc. Color RGB is converted into one dimension, a total of $8 \times 8 \times 8=512$ bins. Among them,

$$r = image[(y * W + x) * 3] \gg R_SHIFT \tag{5}$$

$$g = image[(y * W + x) * 3 + 1] \gg G_SHIFT \tag{6}$$

$$r = image[(y * W + x) * 3 + 2] \gg R_SHIFT \tag{7}$$

Here the R_SHIFT, G_SHIFT, B_SHIFT macros are defined as 5, shifted 5 bits to the right, each R, G, B value divided by 32 is mapped to the corresponding 8 bins. 0-31 maps to bins1, 32-63 maps to bins2. 224-255 maps to bins8. That is to say, for each RGB pixel value, it can be mapped to a unique index by calculation, according to the index Accumulate, accumulate the corresponding kernel density weights, and calculate the color histogram [21], [22]. Take the original image of the edge part with $r = 0.6$ as an example, as shown in Fig. 7.

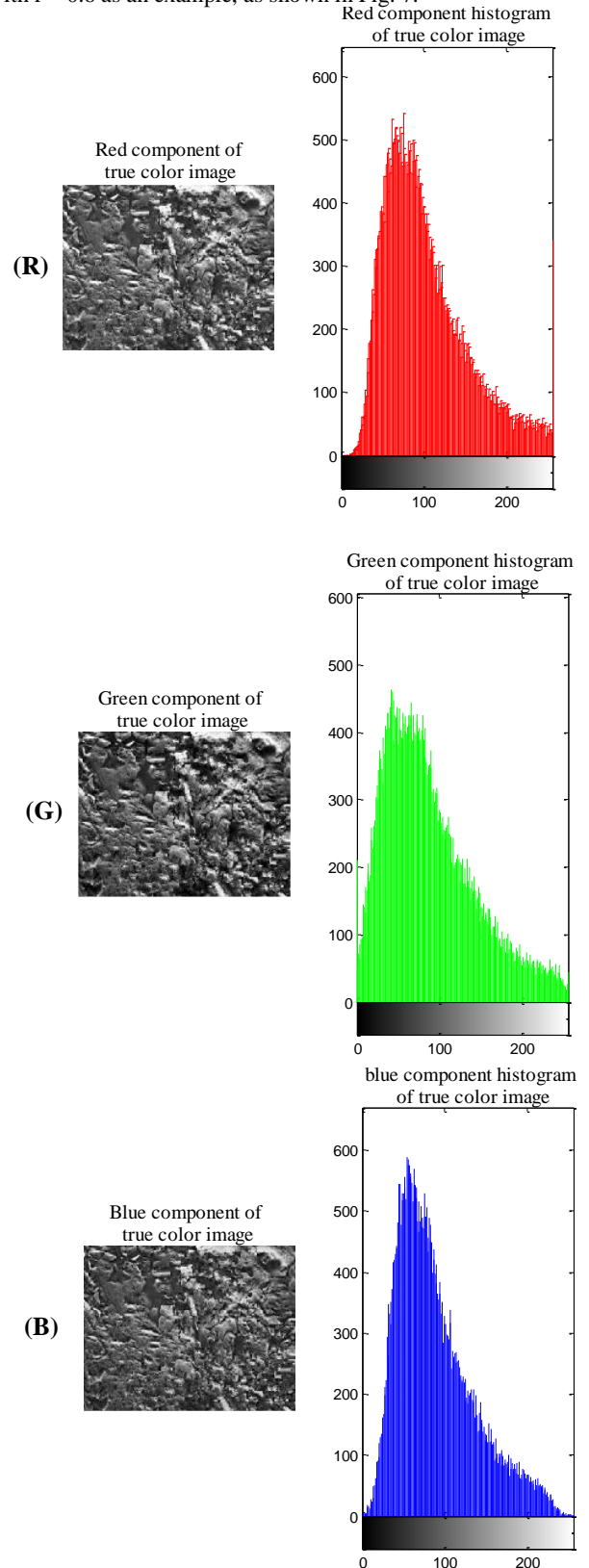


Fig.7. Marginal part R = 0.6 RGB histogram

4.1 Principle of counting box dimension

Based on the extraction of RGB color features, the three color channels of different parts, different alkalinity, and different elements are extracted separately [23]. This article takes the 7 elements of the edge part of the pellet phase and the alkalinity 0.6 as an example, as shown in the Fig. 8 shown.

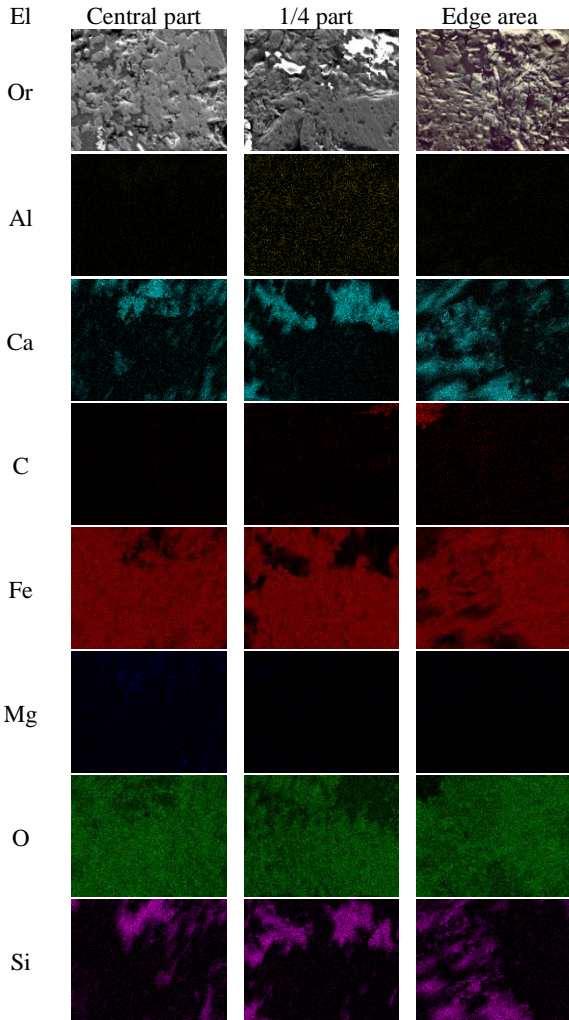


Fig.7. Image of 7 elements in pellet phase with R = 0.6

In this paper, the pellets of 7 elements are extracted by RGB primary colors, and the color features of R, G, and B are compared in Fig. 9, Fig.10 and Fig.11 [24].

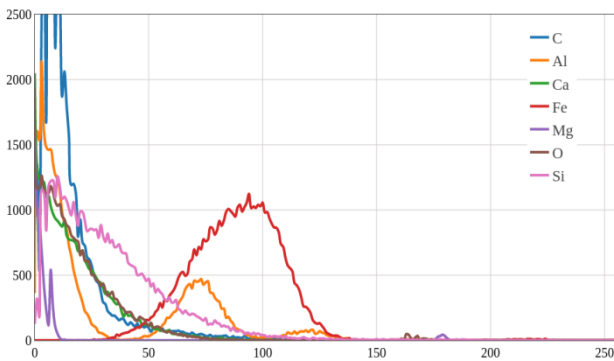


Fig.9. Comparison of R color characteristics of different elements.

Comparing Fig. 9, Fig.10 and Fig.11, it is found that the color characteristics of different elements are obviously different, and

the three color characteristics of the same element also have different situations. By comparing different elements horizontally and different color characteristics vertically, for pellets containing different metals Summing up the following conclusions (Table 3):

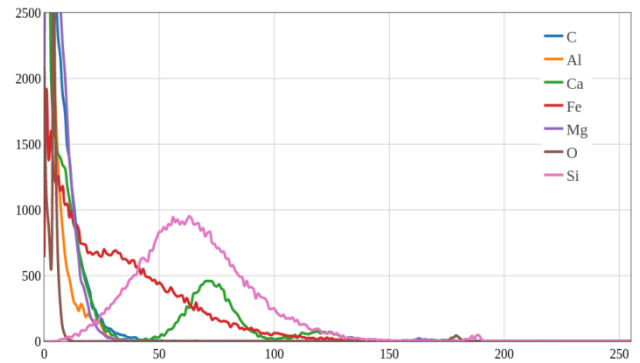


Fig.10. Comparison of G color characteristics of different elements.

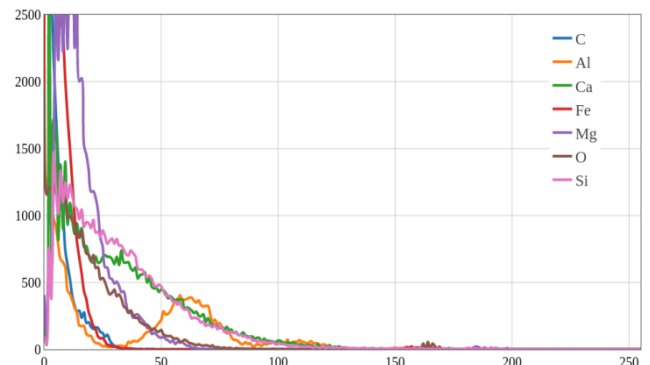


Fig.11. Comparison of B color characteristics of different elements.

Table 3. Conclusion

Metal contained	Conclusion
Original	The shape and size of the color histogram of the three primary colors are the same, and all have peaks
Al	The histogram shape of red and green is similar, and there are three peaks
C	The red histogram has the largest area and all colors are similar in shape, Histograms of all three colors contain two peaks
Fe	The highest point of red wave is about 100, and its area is the largest; At the same time, green and blue are similar in shape and have no wave crest
Ca	The red area is the smallest, and there is no wave crest; Green is similar to blue in shape, with 4 to 5 peaks
Mg	Red, green area is relatively small, and the three colors have no peak
O	The highest green peak is about 75, and there is no peak in the blue and red histogram
Si	Red and blue areas are the largest and similar, and none of the three colors have their peaks

Therefore, RGB color histogram can be used as a method to distinguish the main features of ore phase elements in pellets.

5. Conclusion

In this paper, we have applied gray level co-occurrence matrix

algorithm and box counting dimension algorithm to extract and analyze the feature information, texture color, RGB color histogram, basicity feature of pellet mineral phase, fractal feature and color feature. The different basicity, location and element obtained different feature information, and finally got the texture feature-recognize different alkalinity, fractal feature--recognize different parts, color feature--recognize different elements, and provide the main feature extraction of pellet mineral phase Theoretical basis.

The above three algorithms are used to solve the texture feature parameters for identifying alkalinity, the classification feature parameters for identifying parts, and the RGB image features for identifying colors. Therefore, by using image pattern recognition technology to test pellets in the future, pellets can be analyzed Screening to effectively reduce the consumption of metallurgical raw materials, save time and cost, improve metallurgical performance, etc., provides a theoretical basis for improving the iron-making effect of iron and steel enterprises.

Acknowledgements

This work is supported by the National Natural Science Foundation of China under Grant 51674121.

References

- [1] Yang A, Zhuansun Y, Shi Y, et al. IoT System for Pellet Proportioning Based on BAS Intelligent Recommendation Model[J]. IEEE Transactions on Industrial Informatics, 2019. DOI: 10.1109/TII.2019.2960600
- [2] Prasad R, Venugopal R, Kumarwamidhas L A, et al. Effect of microwave heat hardening on microstructure and strength of coke composed iron ore pellet[J]. Materials Today: Proceedings, 2020. DOI:10.1016/j.matpr.2020.02.267
- [3] Fu X J, Chu M S. Experimental study on preparation of oxidized Barun iron ore pellets with boron-bearing iron concentrate addition[J]. Dongbei Daxue Xuebao/journal of Northeastern University, 2015, 36(1):52-56. DOI: 10.3969/j.issn.1005-3026.2015.01.012
- [4] Chen S Y, Chu M S, Tang J, et al. Effects of pre-oxidation on phase composition and microstructure of vanadium titano-magnetite[J]. Dongbei Daxue Xuebao/journal of Northeastern University, 2013, 34(4):536-541. DOI: 10.1080/00224545.1980.9924284
- [5] FAN Jian-jun, GUO Yu-feng, ZANG Long, et al. Effect of basicity on properties of pellets produced by ultra fine-sized iron concentrate[J]. Journal of Iron and Steel Research, 2019, 31(5): 440-445. DOI: 10.13228/j.boyuan.issn1001-0963.20180285
- [6] Yang Han, Aimin Yang, Yuzhu Zhang. BAS intelligent recommendation model for optimum proportion of pellet raw materials[J]. Chinese Journal of Scientific Instrument, 2019, 40(09):246-254. DOI: 10.19650/j.cnki.cjsi.J1905266
- [7] Jianqiao S, Jiaying D, Xianzhu Z. Study on Relationship between Gear Wear Characteristics and Performance Based on Gray Co-occurrence Matrix[J]. Tool Engineering, 2018, 052(002):84-87. DOI: 10.3969/j.issn.1000-7008.2018.02.019
- [8] Tian, Youwen, Cheng, Yi, Wang, Xiaoqi, et al. Recognition method of insect damage and stem/calyx on apple based on hyperspectral imaging[J]. transactions of the chinese society of agricultural engineering, 2015, 31(4):325-331. DOI: 10.3969/j.issn.1002-6819.2015.04.046
- [9] Yu C, Ling T U, Li-Fang W U. Face Liveness Detection using Gray Level Co-Occurrence Matrix and Wavelets Analysis in Identity Authentication[J]. Journal of Signal Processing, 2014, 000(007):830-835. DOI: 10.3969/j.issn.1003-0530.2014.07.011
- [10] Jie Z, Shuo-Ran G, Long W, et al. Three-dimensional Reconstruction Of Brain CT Images And Study On Its Texture Characteristics[J]. Laser Journal, 2014(6): 62-65. DOI: 10.3969/j.issn.0253-2743.2014.06.062
- [11] LIU Kang, CHEN Xiao-lin, LIU Yan-jun, et al. Vane pump assembly quality detection based on gabor and gray level co-occurrence matrix hybrid characteristics[J]. Chinese Journal of Liquid Crystals and Displays, 2018, 33(11): 936-942. DOI: 10.3788/JYXS20183311.0936
- [12] Tan J, Gao Y, Liang Z, et al. 3D-GLCM CNN: A 3-dimensional gray-level co-occurrence matrix based CNN model for polyp classification via CT colonography[J]. IEEE Transactions on Medical Imaging, 2019(39): 2013-2024. DOI: 10.1109/TMI.2019.2963177
- [13] Sharma M, Pachori R B, Acharya U R. A new approach to characterize epileptic seizures using analytic time-frequency flexible wavelet transform and fractal dimension[J]. Pattern Recognition Letters, 2017, 94: 172-179. DOI: 10.1016/j.patrec.2017.03.023
- [14] Martos F J, Lapuerta M, Expósito J J, et al. Overestimation of the fractal dimension from projections of soot agglomerates[J]. Powder Technology, 2017, 311: 528-536. DOI: 10.1016/j.powtec.2017.02.011
- [15] Mohammed M A, Al-Khateeb B, Rashid A N, et al. Neural network and multi-fractal dimension features for breast cancer classification from ultrasound images[J]. Computers & Electrical Engineering, 2018, 70: 871-882. DOI: 10.1016/j.compeleceng.2018.01.033
- [16] Sahu A, Priyadarshi A. On the box-counting dimension of graphs of harmonic functions on the Sierpiński gasket[J]. Journal of Mathematical Analysis and Applications, 2020: 124036. DOI: 10.1016/j.jmaa.2020.124036
- [17] Niu Z, Jiao L, Chen S, et al. Surface Quality Evaluation in Orthogonal Turn-Milling Based on Box-Counting Method for Image Fractal Dimension Estimation[J]. nanomanufacturing & metrology, 2018:1-6. DOI: 10.1007/s41871-018-0015-x
- [18] Deng K, Pan D, Li X, et al. Spark testing to measure carbon content in carbon steels based on fractal box counting[J]. Measurement, 2019, 133: 77-80. DOI: 10.1016/j.measurement.2018.10.004
- [19] Mehta D, Sridhar S, Sotnychenko O, et al. Vnect: Real-time 3d human pose estimation with a single rgb camera[J]. ACM Transactions on Graphics (TOG), 2017, 36(4): 1-14. DOI: 10.1145/3072959.3073596
- [20] Wang P, Li W, Ogunbona P, et al. RGB-D-based human motion recognition with deep learning: A survey[J]. Computer Vision and Image Understanding, 2018, 171: 118-139. DOI: 10.1016/j.cviu.2018.04.007
- [21] Jia H, Sun K, Song W, et al. Multi-Strategy Emperor Penguin Optimizer for RGB Histogram-Based Color Satellite Image Segmentation Using Masi Entropy[J]. IEEE Access, 2019, 7: 134448-134474. DOI: 10.1109/ACCESS.2019.2942064
- [22] Wang P, Li W, Ogunbona P, et al. RGB-D-based human motion recognition with deep learning: A survey[J]. Computer vision and image understanding, 2018, 171(JUN.):118-139. DOI: 10.1016/j.cviu.2018.04.007
- [23] Yan W, Zheng-Zheng T U, Ai-Hua Z, et al. Shadow Elimination Algorithm of Combination of RGB Color Feature and Texture Feature[J]. computer technology and development, 2013, 000(010):72-74,79. DOI: 10.3969/j.issn.1673-629X.2013.10.018
- [24] Yu Zhang, Haiqing Tian, Zhe Li, et al. Nitrogen nutrition monitoring of beet canopy based on digital camera image[J]. Transactions of the Chinese Society of Agricultural Engineering, 2018, 034(001):157-163. DOI: 10.11975/j.issn.1002-6819.2018.01.021



Yunxi Zhuansun was born in JiNing, Shandong province, China in 1995, He graduated from the BinZhou University. Now, he is a graduate student of Graduate School of North China University of science and technology, studying in math, mainly researches on numerical calculation and its application.
Email: zhuansunyunxi_ncst@163.com



Wei Zhang is currently studying computational mathematics with the School of Science, North China University of Science and Technology, Hebei, China. His current research interests include data mining and bioinformatics.
Email: zhangwei_ncst@163.com



Jianming Zhi received a bachelor's degree from Taiyuan University of Technology in 2019 and a master's degree from North China University of Technology after 2019. He majored in metallurgical engineering specializing in big data processing in the metallurgical direction. Currently his main research fields and directions are: metallurgical energy conservation and environmental protection.
Email: zhijianming_ncst@163.com



Yang Han is with the College of Metallurgy and Energy, North China University of Science and Technology, Tangshan, Hebei, China. He was born in Jizhou, Hebei, China, in 1987. He received the BS and MS degrees from North China University of Science and Technology in 2010 and 2018, respectively. He is currently a Ph.D. student at North China University of Science and Technology. His main research interests include numerical computation, iron and steel big data, and intelligent computation, etc. Email: hanyang@ncst.edu.cn